ChemBioChem

Research Article
doi.org/10.1002/cbic.202200414

Chemistry Europe
European Chemical Societies Publishing

www.chembiochem.org

VIP *Very Important Paper*

Chemical Proteomics Reveals Protein Tyrosination Extends Beyond the Alpha-Tubulins in Human Cells**

Dmytro Makarov[a] and Pavel Kielkowski*[a]

Tubulin detyrosination-tyrosination cycle regulates the stability of microtubules. With respect to α-tubulins, the tyrosination level is maintained by a single tubulin-tyrosine ligase (TTL). However, the precise dynamics and tubulin isoforms which undergo (de)tyrosination in neurons are unknown. Here, we exploit the substrate promiscuity of the TTL to introduce an *O*-propargyl-L-tyrosine to neuroblastoma cells and neurons. Mass spectrometry-based chemical proteomics in neuroblastoma cells using the *O*-propargyl-L-tyrosine probe revealed previously discussed tyrosination of TUBA4A, MAPRE1, and other non-tubulin proteins. This finding was further corroborated in differentiating neurons. Together we present the method for tubulin tyrosination profiling in living cells. Our results show that detyrosination-tyrosination is not restricted to α-tubulins with coded C-terminal tyrosine and is thus involved in fine-tuning of the tubulin and non-tubulin proteins during neuronal differentiation.

Introduction

Microtubules (MTs) are composed of α- and β-tubulin heterodimers and are essential for function and stability of the cellular cytoskeleton. The defined MTs composition is critical for intracellular transport, mechanical resistance, mitosis and migration.[1] Both α- and β-tubulin are encoded in the human genome in multiple isotypes, which have been observed to be tissue- and cell-type-specific.[2] The heterogeneity of MTs is further extended by numerous post-translational modifications (PTMs) including acetylation, (poly)glutamylation, (poly)glycylation, (poly)amination and tyrosination together called the tubulin code (Figure 1A).[3] The majority of these PTMs are concentrated on the disordered tubulin C-terminus. In most of the α-tubulins, the encoded C-terminal amino acid is tyrosine, which can be cleaved by VASH-SVBP complex or most recently discovered MATCAP carboxypeptidase (Figure 1B).[4] The terminal tyrosine is restored in translation independent manner by tubulin-tyrosine ligase. Regulation of the tyrosination statutes fine-tunes the stability of α- and β-tubulin heterodimer and MTs.[5] The stable MTs induced by paclitaxel show an increased amount of detyrosinated α-tubulin, while

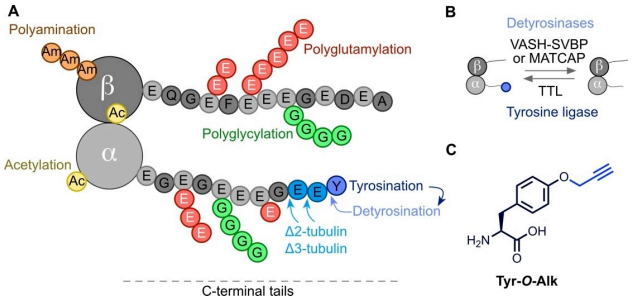

Figure 1. Microtubules detyrosination and tyrosination cycle. A) Tubulin code overview. B) Enzymes involved in detyrosination and tyrosination. C) Structure of the **Tyr-*O*-Alk** probe.

tubulin heterodimers and unstable MTs are characterized by tyrosinated α-tubulin.[5] However, the tyrosinated tubulins are not required for MTs polymerization nor MTs detyrosination is sufficient for their stabilization. The physiological relevance was demonstrated on TTL knockout mice, which die perinatally and display dysregulated development of neuronal networks.[6] The upregulated MTs detyrosination was linked to failing hearts in patients with ischemic cardiomyopathy.[7] On the cellular level, MTs detyrosination is critical for directional transport of chromosomes and governance of interaction between MTs and microtubule-associated proteins (MAPs).[7] Overall tubulin tyrosination was previously analyzed by cell pretreatment with cycloheximide (CHX) to block the protein synthesis and subsequent addition of tritiated tyrosine analogue to track the tyrosine incorporation by radioactivity.[8] Tubulin C-terminus labelling can also be achieved by incorporation of non-natural tyrosine analogues, for example, 3-N_3-L-tyrosine or 3-formyltyrosine.[8] The latter can subsequently react with 7-hydrazino-4-methyl coumarin to provide a fluorescent tag on labelled proteins in living cells. The tubulin (de)tyrosination status is usually identified by PTM-specific antibodies.[8] However, these do not distinguish individual tubulin isotypes. On

[a] *D. Makarov, Dr. P. Kielkowski*
LMU München, Department of Chemistry
Institute for Chemical Epigenetics – Munich (ICEM)
Würmtalstrasse 201, 81375 Munich (Germany)
E-mail: pavel.kielkowski@cup.lmu.de

[**] *A previous version of this manuscript has been deposited on a preprint server (https://www.biorxiv.org/content/10.1101/2022.07.02.498566v1).*

Supporting information for this article is available on the WWW under https://doi.org/10.1002/cbic.202200414

This article is part of the Special Collection ChemBioTalents2022. Please see our homepage for more articles in the collection.

the other hand, liquid chromatography (LC) with mass spectrometry (MS)-based detection of tyrosinated and detyrosinated peptide fragments is not feasible due to the very high complexity of C-terminal peptide PTMs.

Here, we report an MS-based chemical proteomics approach to decipher the composition of post-translationally tyrosinated proteins in living cells. The approach is based on the low substrate selectivity of the TTL. The TTL's active site was shown to be able to accommodate various tyrosine analogues.[9] In contrast, modified tyrosines are poor substrates for translation machinery. Thus, avoiding unspecific labelling of bulk proteins.

Results and Discussion

To initiate the study, we designed and applied the *O*-propargyl-L-tyrosine (**Tyr-*O*-Alk**, Figure 1C), which was previously tested in *in vitro* tubulin C-terminus modification catalyzed by the TTL.[9] The **Tyr-*O*-Alk** was synthesized in three steps from L-tyrosine (Figure S1). First, the cytotoxicity of the **Tyr-*O*-Alk** was evaluated on SH-SY5Y neuroblastoma cells to show no toxicity up to 2 mM final concentration of the probe in cell culture media (Figure S2). Second, a series of in-gel experiments were carried out to optimize the labelling efficiency and to test the probe's fidelity (Figure 2A). The **Tyr-*O*-Alk** treatment times of SH-SY5Y cells were optimized. To evaluate the extent of **Tyr-*O*-Alk** incorporation, the probe-treated cells were lysed and reacted under copper-catalyzed azide-alkyne cycloaddition (CuAAC) conditions with rhodamine-PEG$_3$-azide (TAMRA-N$_3$). The labelled proteins were separated using sodium dodecyl sulfate-polyacrylamide gel (SDS-PAGE) electrophoresis and rhodamine fluorescence was scanned. The successful protein labelling was observed already between 8 to 16 hours after the addition of the 300 μM **Tyr-*O*-Alk** into cell culture media but further increased for a total of two days (Figure 2B).

Interestingly, the strongest fluorescence band exhibiting time-dependent labelling was observed at around 50 kDa, suggesting the labelling of tubulins. In parallel, probe concentration was tested to reveal that already 200 μM final concertation provides bright fluorescent bands (Figure S3).

Next, to confirm the translation-independent incorporation of **Tyr-*O*-Alk** in proteins, the SH-SY5Y cells were pre-treated with CHX to block the protein synthesis before **Tyr-*O*-Alk** probe addition (Figure 2C). Indeed, we observed only a decrease in fluorescence intensity related to the decrease of total α-tubulin (Figure S4). This confirms the introduction of **Tyr-*O*-Alk** as protein PTM rather than via ribosomal protein synthesis. Furthermore, a competition experiment between the probe and natural tyrosine was performed to test the probe's fidelity. Indeed, the probe labelling was clearly diminished with an increasing amount of natural tyrosine (Figure 2D and Figure S5). Next, the tubulin fraction was isolated by taxol-induced depolymerization-polymerization of MTs from **Tyr-*O*-Alk** treated SH-SY5Y cells.[8b,10] The single probe-specific fluorescent band was observed in the tubulin fraction, corroborating the fidelity of the probe (Figure 2E). Tubulin fraction isolation was tested by western blot using the anti-TUBA antibody. Finally, the turnover of the **Tyr-*O*-Alk** probe was examined by treatment of the SH-SY5Y cells with the probe, followed by cell culture media exchange without the probe. Surprisingly, we observed a rather

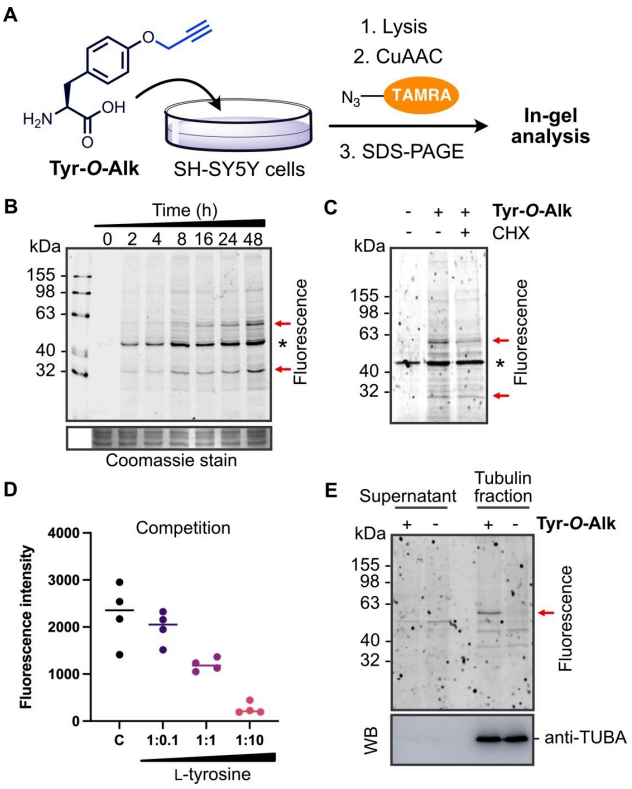

Figure 2. In gel analysis of **Ty-O-Alk** protein metabolic labelling in SH-SY5Y cells. A) The overall metabolic labelling strategy. B) Time-dependent labelling using the **Tyr-O-Alk** probe (300 μM). Cells were harvested at indicated time points after addition of the probe. C) The cells were pre-treated with CHX for 30 min before addition of the **Tyr-O-Alk** probe and incubation for 24 h. This excludes the incorporation of the probe via ribosomal translation machinery. D) The cells were treated with a constant final concentration of the **Tyr-O-Alk** probe and further supplemented with the increasing amount of L-tyrosine as indicated. E) In-gel fluorescence of the isolated tubulin fraction reveals a single specific band at around 55 kDa. Abbreviation: C : control, only **Tyr-O-Alk** probe treated cells. WB : Western blot. B), C) and E) The red arrows point to a fluorescent band stemming from estimated tubulin (~50 kDa) and MAPRE1 (~30 kDa) labelling. An asterisk marks unspecific TAMRA-N$_3$ labelling.

Pavel Kielkowski studied chemistry at University of Chemistry and Technology in Prague and continued with his PhD work on artificial nucleosides, nucleotides and nucleic acids with Prof. Michal Hocek at the IOCB in Prague and Charles University. In 2014, he joined the group of Prof. Stephan Sieber at the TUM, where he developed chemical proteomics approaches for analysis of protein AMPylation. Since 2019 he has been an independent research group leader at the LMU Munich. His laboratory focuses on chemical biology of protein post-translational modifications during neuronal differentiation and neurodegeneration.

slow replacement of incorporated propargyl tyrosine by natural tyrosine, only after 24 h, there was no observable band present (Figure S6). Together, these experiments support the efficient incorporation of **Tyr-*O*-Alk** in tubulins as PTM.

To decipher the composition of tubulin isoforms labelled by the **Tyr-*O*-Alk** probe, we continued with MS-based chemical proteomics. Recently, we have established an efficient chemical proteomics enrichment approach called SP2E.[11] The SP2E workflow uses the carboxylate-modified magnetic beads to clean up the proteins after the click chemistry with biotin-N_3. During this process, the carboxylate-modified magnetic beads are aggregated together with proteins after addition of an organic solvent such as ethanol or acetonitrile.[12] In the next step, the proteins are eluted from the carboxylate magnetic beads and transferred on streptavidin-coated magnetic beads. The biotin-labelled proteins are enriched and digested by trypsin. The resulting peptide mixtures corresponding to the enriched probe-modified proteins are collected and analyzed via LC-MS/MS. In parallel, the same procedure is carried out with control cells to be able to abstract the background, which is composed of non-specifically enriched proteins (Figure 3A). We have utilized the SP2E workflow to enrich **Tyr-*O*-Alk** labelled proteins from SH-SY5Y cells in quadruplicates using data-independent acquisition (DIA).[13] Indeed, analysis of resulting MS spectra by DIA-NN[13] via label-free quantification (LFQ)[13] confirmed the significant enrichment of α-tubulin isoforms including TUBA1C and TUBA4A (Figure 3B). To gain more confidence in the identification of the highly similar tubulin isoforms, we have revised the peptides assigned to the tubulin isoforms together with corresponding MS2 spectra (Table S1). This analysis showed that at least 2 unique peptides were found for each α-tubulin isoform. The TUBA4A isoform does not encode the C-terminal tyrosine resembling the detyrosinated tubulin when translated. However, TUBA4A was speculated to be possibly tyrosinated, which is now corroborated by our results. Surprisingly, several non-tubulin proteins were found to be significantly enriched as well. This group contains the microtubule-associated protein RP/EB family member 1 (MAPRE1 also called EB1) a marker of the microtubule plus-end, which regulates the dynamics of the microtubule cytoskeleton.[14] MAPRE1 is involved in a mitotic spindle positioning and recruiting the CLIP170 to MTs (+)-end.[14] Importantly, sequence analysis of this 30 kDa protein contains the α-tubulin-like C-terminus coding the terminal tyrosine adjacent to two glutamates (PQEEQ**EEY**). This would suggest a potential detyrosination-tyrosination cycle, as discussed in the literature.[15] The retrospective analysis of the in-gel fluorescence labelling shows clear time-dependent labelling of a protein at around 30 kDa (Figure 2B). Another microtubule-associated protein TUBGCP5 was significantly enriched based on the one unique peptide found in four probe-treated replicates but not in the controls suggesting TUBGCP5 modification by the probe. Some other non-tubulin proteins were significantly and consistently enriched (as well in the following experiments in iNGNs), such as MARCKS, DCTN3 and LSM6. From these, the MARCKS and DCTN3 are proteins with a role in cytoskeleton organization. Although it is assumed that the **Tyr-*O*-Alk** probe is incorporated into proteins and, in particular, in α-tubulin by TTL, it cannot be excluded that other proteins possess similar catalytic function. For example, He et al. described the tRNA synthetases to act as aminoacyl transferases modifying the lysine side chain amino group.[16] In parallel, the **Tyr-*O*-Alk** probe-treated lysates were processed by SP3[17] for whole proteome MS analysis to exclude the translation-dependent

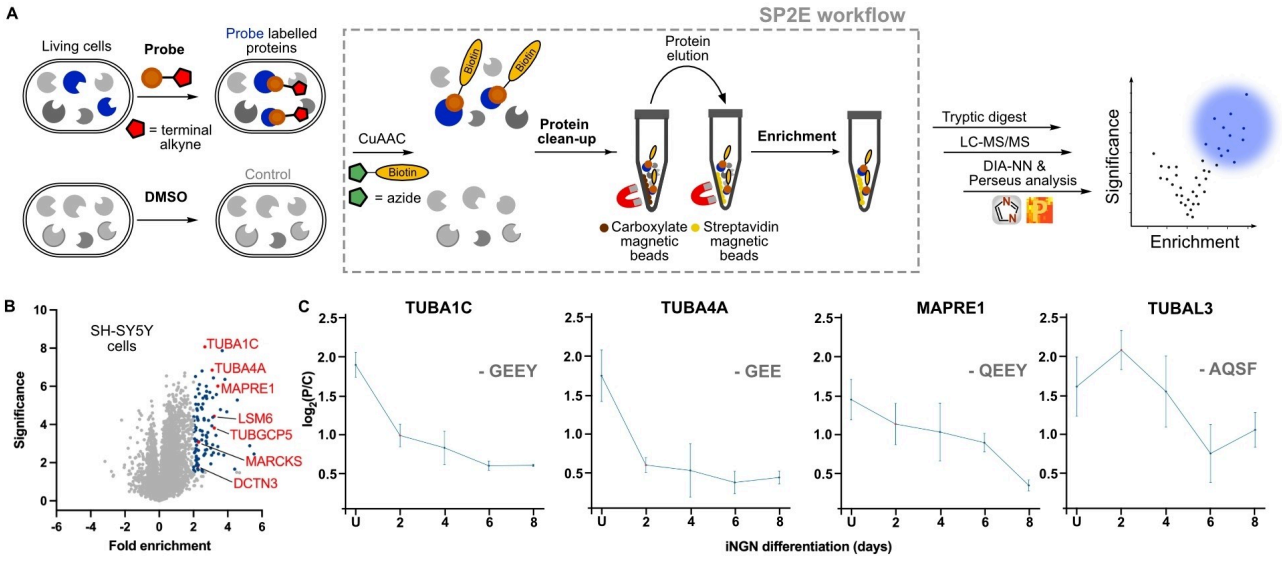

Figure 3. Mass spectrometry-based chemical proteomics of SH-SY5Y and iNGN cells uncovered the scope of protein tyrosination. A) Overview of MS-based chemical proteomics workflow using the SP2E. B) Volcano plot visualizing the enrichment of **Tyr-*O*-Alk** labelled proteins from SH-SY5Y cells; Blue dots are significantly enriched proteins with at least 4-fold enrichment. $n = 4$, fold enrichment ($\log_2$(**Tyr-*O*-Alk**/control), significance ($-\log_{10}$(*p*-value)). C) Fold change of tyrosination on selected proteins during iNGNs neuronal differentiation showing tyrosination/detyrosination cycle of TUBA4A and MAPRE1. The isoform encoded C-terminal sequences are added for comparison. Points represent the mean of four replicates (C: control; P: **Tyr-O-Alk** probe treated) with standard error of the mean (SEM).

stochastic incorporation of the probe into a primary amino acid sequence of proteins. The resulting MS spectra were searched for the presence of peptides containing tyrosine with *O*-propargyl as variable modification. In both control and **Tyr-*O*-Alk** treated cells on average only 42.5 and 33 modified proteins were found from an average of 38606 and 37291 total peptides, respectively (Table S2 and Figure S7). Thus, suggesting the **Tyr-*O*-Alk** is not incorporated into proteins by ribosomal translation machinery but rather post-translationally. The direct identification of the C-terminal *O*-propargyl tyrosine on tubulins was unlikely as it is challenged by additional C-terminal PTMs exploding the number of possible combinations, which exceed the computational capacity. The whole proteome analysis also revealed that TUBA1C and TUBA4A were the only identified α-tubulins. With the established **Tyr-*O*-Alk** labelling and MS-based chemical proteomics workflow, we moved towards the application of the method to determine the dynamics of protein tyrosination during neuronal differentiation.

The neuronal cells are characterized by their strong polarization of the cell body containing dendrites, axons and synapses. The neuronal cytoskeleton is responsible for the maintenance of this polarization, it supports neuronal migration during cortex development and provides avenues for cellular trafficking.[18] The composition of tubulin isoforms is known to play a role during neuronal differentiation. However, it was previously not possible to link the tubulin isoforms with the corresponding tyrosination status. We applied the **Tyr-*O*-Alk** probe to determine protein tyrosination status during neuronal differentiation of human induced pluripotent stem cells (hiPSCs). To streamline this process, we leveraged from fast (4 days) differentiation of hiPSCs engineered with doxycycline-inducible Neurogenin-1 and −2 cassette (iNGNs).[19] To test the feasibility of our approach in iNGNs, they were treated with **Tyr-*O*-Alk** at four different time points during differentiation into mature neurons (Figure S8). Similar to SH-SY5Y cells, the fluorescent band at around 50 kDa was present, likely corresponding to the tubulins (Figure S8). In addition, we observed a clear change in fluorescence intensity of the 30 kDa band during iNGNs differentiation (Figure S8). Thus, we proceeded with the SP2E enrichment of **Tyr-*O*-Alk** labelled proteins using the trifunctional linker (containing 5/6-TAMRA-N_3-biotin moieties) instead of the biotin-N_3. In contrast to the previous MS experiments, enriched proteins were eluted from streptavidin magnetic beads using the SDS-PAGE loading buffer. Fluorescence imaging of the gel showed the labelling in a region around 30 kDa. The subsequent western blot of these enriched proteins and staining with the anti-MAPRE1 antibody showed the presence of MAPRE1 protein pool in probe-treated cells 2 days after doxycycline-induced neuronal differentiation (Figure S9). Next, the MS-based chemical proteomics was performed using the small-scale 96-well plate format SP2E workflow, starting with 100 μg protein. In total, we have collected the cells at five time points during the iNGNs differentiation and maturation. We have observed a decrease in overall tubulin tyrosination on TUBA1C, TUBA4A and MAPRE1 during the neuronal differentiation (Figure 3C and Figure S10). Moreover, tubulin alpha chain-like 3 (TUBAL3) protein was identified, showing a different pattern. Despite the high sequence similarity with α-tubulins (>75%), the TUBAL3C-terminus lacks the -EEY motive. Several other non-tubulin but cytoskeleton-associated proteins were significantly enriched suggesting their tyrosination including dynactin subunit 3 (DCTN3), alpha-tubulin N-acetyltransferase 1 (ATAT), MARCKS-related proteins MARCKS and MARCKSL1. Surprisingly, a cytosolic U6 snRNA-associated Sm-like protein Lsm6 (LSM6) was consistently enriched at all time points during the iNGNs differentiation (Figure S10). SP2E enrichment experiment in iNGNs was complemented by whole proteome analysis. This confirmed the identity of the neuronal cells and also aided estimation of the trends in tyrosination stoichiometry and thus dynamics. In general, there is a strong increase in total tubulin isoforms expression (Figure S11). The same trend was found for the MAPRE1 explaining the above-described observation using the western blot as the read-out. It was possible to detect MAPRE1 after enrichment with anti-MAPRE1 antibody only in two-day differentiated iNGNs, because of the sufficient absolute amount of tyrosinated MAPRE1 in the lysate. While the MAPRE1 tyrosination (fold enrichment) mildly decreases after two days, there is at the same time a dramatic increase in MAPRE1 protein expression (Figure 3C and Figures S11, S12). The tyrosination status of the proteins correlates well with the expression of the TTL, which is lower than that of carboxypeptidases responsible for tyrosine removal (VASH1 and MATCAP) (Figure S12). Apart from the enriched α-tubulin isoforms, the whole proteome analysis identified the protein group contacting TUBA1A, TUBA3C, TUBA3D and TUBA3E. Together, these experiments provide evidence of significant changes in tyrosination status during neuronal differentiation on tubulin and non-tubulin proteins.

To visualize the probe distribution and incorporation within the SH-SY5Y cells, the **Tyr-*O*-Alk** probe was used for fluorescence imaging (Figure 4A). Control or probe-treated cells were washed to remove excess of the probe, after fixation and permeabilization, they were incubated with TAMRA-N_3 under CuAAC conditions. The strong labelling in the probe-treated cells was observed, with a negligible background in control. Colocalization with TUBA and MAP2 showed partial overlap, which is in line with the fact that tyrosinated tubulins are mostly present in cells as dimers, which are not polymerized in microtubules.

Finally, we were interested in whether it is possible to further utilize the low substrate selectivity of TTL to introduce other functional groups in living cells. The selected *O*-(2-nitrobenzyl)-L-tyrosine (**ONBY**) was added together with **Tyr-*O*-Alk** to the cells in different ratios.

The final concentration of **Tyr-*O*-Alk** was kept constant. This setup resulted in the competition between the two unnatural tyrosines, which was then analyzed after CuAAC with TAMRA-N_3 and fluorescence scanning of the SDS-PAGE (Figure 4B and Figure S13). The MTs incorporated ONBY tubulin might be further used to probe the MTs' interactions with MAPs. The nitrobenzyl residue can be removed by UV-light irradiation, enabling modulation of the tyrosination function in the living cells.[20]

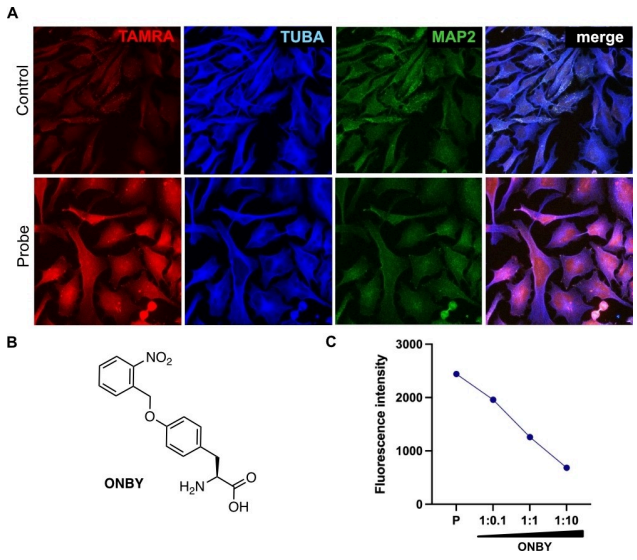

Figure 4. Fluorescence imaging and incorporation of sterically hindered tyrosine derivative. A) Fluorescence imaging of **Tyr-*O*-Alk** treated and control SH-SY5Y cells. B) ONBY structure. C) In-gel analysis of the competition experiment between **Tyr-*O*-Alk** and ONBY in SH-SY5Y cells. The fluorescence band at around 55 kDa was quantified. P – only **Tyr-*O*-Alk** treated cells.

Conclusion

A straightforward approach for chemical proteomic analysis of protein tyrosination in living cells based on the metabolic labelling using the **Tyr-*O*-Alk** probe was developed. Our method enables for the first time to profile tyrosinated tubulin isoforms during neuronal differentiation and strongly suggests that tyrosination is not restricted to α-tubulins. We have confirmed disputed tyrosination of microtubule-associated protein MAPRE1 and TUBA4A as well as on other non-tubulin proteins. Microtubules are critical for mechanical resistance of the cells and intracellular trafficking, the hallmarks of cancer research and neurodegeneration, respectively. Further research in this direction enabled by the reported strategy will be carried out in our laboratory to determine the pathophysiological relevance of protein tyrosination.

Experimental Section

Cell treatment and harvest. SH-SY5Y or iNGN cells were treated with the stock solution of **Tyr-*O*-Alk** (H_2O:1 M NaOH 2:1, 144 mM, sterile filtered), the final concentration in culture media was 0.3 mM. Unless otherwise stated, the cells were treated with the probe for 24 h. After the incubation, the medium was removed, and the cells were washed once with 5 mL of a phosphate-buffered saline solution (PBS). After removing PBS from a dish, cells were scraped with 1 mL of PBS, and transferred to a 1.5 mL tube. The cell suspension was centrifuged at 4 °C at 100 rcf to obtain the cell pellet.

Cell lysis. The cell pellet was reconstituted in 300 µL of a lysis buffer (1% NP40, 0.2% SDS in 25 mM HEPES, 7.5 pH) by sonication with an ultrasonic tip in 1 s on/1 s off cycles at 20% intensity for 10 s of total time. The solution was clarified by centrifugation at 4 °C at 14000 rcf for 15 min.

Small-scale SP2E workflow. Lysates containing 100 µg of proteins were diluted to 19 µL with lysis buffer (1% NP40, 0.2% SDS in 25 mM HEPES, 7.5 pH). For each sample, 0.2 µL Biotin-N_3 (10 mM in DMSO), 0.2 µL of TCEP (100 mM in H_2O), and 0.125 µL TBTA (16.7 mM in DMSO) was added, vortexed, spun down, and supplemented with 0.4 µL of $CuSO_4$ (50 mM in H_2O) to initiate the reaction. The reaction mixture was incubated at r.t. while shaking at 450 rpm for 1.5 h. After completion of the click reaction, each sample was diluted with 60 µL of 8 M urea. A 1:1 mixture of hydrophobic and hydrophilic carboxylate-coated magnetic beads (100 µL) was washed three times with 100 µL MS-grade H_2O, and the reaction mixture was placed on the beads, diluted with 100 µL of absolute ethanol and vortexed. The suspension was incubated at r.t. while shaking at 950 rpm for 5 min. Afterward, the supernatant was discarded, and the beads were washed thrice with 150 µL of 80% ethanol in H_2O and once with 150 µL acetonitrile (LC-MS). Proteins were eluted separately by adding 60 µL of 0.2% SDS in PBS. For this, beads were resuspended and incubated for 5 min at 40° C and 950 rpm. The supernatant was directly transferred onto 50 µL equilibrated streptavidin-coated magnetic beads (3 times prewashed with 100 µL 0.2% SDS in PBS). The elution step was repeated twice and the combined beads mixture was incubated at r.t. while shaking at 800 rpm for 1 h. The supernatant was discarded, and the beads were washed three times with 150 µL 1% NP-40 in PBS, twice with 150 µL 6 M Urea in H_2O, and twice with 500 µL MS-grade H_2O. After each round of washing, the beads were incubated at r.t. while shaking at 800 rpm for 1 min. The rinsed beads mixtures were resuspended in 50 µL 50 mM TEAB, and the proteins were digested overnight at 37 °C by adding 1.5 µL sequencing grade trypsin (0.5 mg/mL). The following day, the beads were washed twice with 20 µL of 50 mM TEAB buffer and twice with 20 µL 0.5% FA, and the wash fractions were collected and combined. The beads were incubated for 5 min at 40 °C and 600 rpm for each washing step. The combined washed fractions were acidified by adding 0.9 µL formic acid (FA) and transferred to MS vials.

MS acquisition and analysis. MS measurements were performed on an Orbitrap Eclipse Tribrid Mass Spectrometer (Thermo Fisher Scientific) coupled to an UltiMate 3000 Nano-HPLC (Thermo Fisher Scientific) via an EASY-Spray source (Thermo Fisher Scientific) and FAIMS interface (Thermo Fisher Scientific). First, peptides were loaded on an Acclaim PepMap 100 µ-precolumn cartridge (5 µm, 100 Å, 300 µm ID×5 mm, Thermo Fisher Scientific). Then, peptides were separated at 40 °C on a PicoTip emitter (noncoated, 15 cm, 75 µm ID, 8 µm tip, New Objective) that was *in-house* packed with Reprosil-Pur 120C18-AQ material (1.9 µm, 150 Å, Dr. A. Maisch GmbH). The DIA duty cycle consisted of one MS1 scan followed by 30 MS2 scans with an isolation window of the 4 m/z range, overlapping with an adjacent window at the 2 m/z range. MS1 scan was conducted with Orbitrap at 60000 resolution power and a scan range of 200–1800 m/z with an adjusted RF lens at 30%. MS2 scans were conducted with Orbitrap at 30000 resolution power, RF lens was set to 30%. The precursor mass window was restricted to a 500–740 m/z range. HCD fragmentation was enabled as an activation method with a fixed collision energy of 35%. FAIMS was performed with one at 45 V compensation voltage (CV) for both MS1 and MS2 scans. Standalone DIA-NN software under version 1.8.1 was used for protein identification and quantification. First, a spectral library was predicted *in silico* by the software's deep learning-based spectra, RTs and IMs prediction using Uniprot *H. sapiens* decoyed FASTA (canonical and isoforms – May 2022). FASTA digest for library-free search/library generation option was enabled for this. Spectral library prediction was performed in 4 batches of

10 samples each to decrease the computational load. Second, all samples (40) were processed together without spectral library generation, with a match between runs (MBR) option and precursor FDR level set at 1%. DIA-NN search settings: Library generation was set to smart profiling, Quantification strategy - Robust LC. The mass accuracy the MS1 accuracy, and the scan window were set to 0 to allow the software to identify optimal conditions. The precursor m/z range was changed to 500–740 m/z to fit the measuring parameters. Carbamidomethylation was set as a fixed modification, oxidation of methionine and N-term acetylation were set as variable modifications. On the contrary, the small-scale samples of the 96-well plate were calculated without carbamidomethylation as a fixed modification. Statistical analysis of the DIA-NN result table "report.pg_matrix.csv" was done with Perseus 1.6.10.43.

Mass spectrometry-based proteomics data have been deposited at ProteomeXchange. The accession number is PXD037402.

Acknowledgements

This work was funded by Liebig fellowship (Fonds der chemischen Industrie) and LMUexcellent Junior Research Fund to P.K. We are grateful for generous support from SFB 1309 – 325871075 (Deutsche Forschungsgemeinschaft). Open Access funding enabled and organized by Projekt DEAL.

Conflict of Interest

The authors declare no conflict of interest.

Data Availability Statement

The data that support the findings of this study are openly available in ProteomeXchange at https://www.ebi.ac.uk/pride/, reference number PXD037402.

Keywords: chemical proteomics · microtubules · neuronal differentiation · protein modifications · tyrosination

[1] a) C. P. Garnham, A. Roll-Mecak, *Cytoskeleton* **2012**, *69*, 442–463; b) P. W. Baas, A. N. Rao, A. J. Matamoros, L. Leo, *Cytoskeleton* **2016**, *73*, 442–460.
[2] a) M. A. Tischfield, E. C. Engle, *Biosci. Rep.* **2010**, *30*, 319–330; b) T. J. Hausrat, J. Radwitz, F. L. Lombino, P. Breiden, M. Kneussel, *Dev. Neurobiol.* **2021**, *81*, 333–350.
[3] a) C. Janke, M. M. Magiera, *Nat. Rev. Mol. Cell Biol.* **2020**, *21*, 307–326; b) J. Nieuwenhuis, T. R. Brummelkamp, *Trends Cell Biol.* **2018**, *29*, 80–92; c) A. Roll-Mecak, *Curr. Opin. Cell Biol.* **2019**, *56*, 102–108.
[4] a) C. Aillaud, C. Bosc, L. Peris, A. Bosson, P. Heemeryck, J. V. Dijk, J. L. Friec, B. Boulan, F. Vossier, L. E. Sanman, S. Syed, N. Amara, Y. Couté, L. Lafanechère, E. Denarier, C. Delphin, L. Pelletier, S. Humbert, M. Bogyo, A. Andrieux, K. Rogowski, M.-J. Moutin, *Science* **2017**, *358*, 1448–1453; b) C. Zhou, L. Yan, W. Zhang, Z. Liu, *Nat. Commun.* **2019**, *10*, 3212; c) L. Landskron, J. Bak, A. Adamopoulos, K. Kaplani, M. Moraiti, L. G. van den Hengel, J.-Y. Song, O. B. Bleijerveld, J. Nieuwenhuis, T. Heidebrecht, L. Henneman, M.-J. Moutin, M. Barisic, S. Taraviras, A. Perrakis, T. R. Brummelkamp, *Science* **2022**, *376*, eabn6020.
[5] a) A. E. Prota, M. M. Magiera, M. Kuijpers, K. Bargsten, D. Frey, M. Wieser, R. Jaussi, C. C. Hoogenraad, R. A. Kammerer, C. Janke, M. O. Steinmetz, *J. Cell Biol.* **2013**, *200*, 259–270; b) C. A. Arce, J. A. Rodriguez, H. S. Barra, R. Caputto, *Eur. J. Biochem.* **1975**, *59*, 145–149.
[6] C. Erck, L. Peris, A. Andrieux, C. Meissirel, A. D. Gruber, M. Vernet, A. Schweitzer, Y. Saoudi, H. Pointu, C. Bosc, P. A. Salin, D. Job, J. Wehland, *Proc. Natl. Acad. Sci. USA* **2005**, *102*, 7853–7858.
[7] X. Yu, X. Chen, M. Amrute-Nayak, E. Allgeyer, A. Zhao, H. Chenoweth, M. Clement, J. Harrison, C. Doreth, G. Sirinakis, T. Krieg, H. Zhou, H. Huang, K. Tokuraku, D. S. Johnston, Z. Mallat, X. Li, *Nature* **2021**, *594*, 560–565.
[8] a) H. S. Barra, C. A. Arce, J. A. Rodríguez, R. Caputto, *Biochem. Biophys. Res. Commun.* **1974**, *60*, 1384–1390; b) A. Banerjee, T. D. Panosian, K. Mukherjee, R. Ravindra, S. Gal, D. L. Sackett, S. Bane, *ACS Chem. Biol.* **2010**, *5*, 777–785; c) D. Schumacher, J. Helma, F. A. Mann, G. Pichler, F. Natale, E. Krause, M. C. Cardoso, C. P. R. Hackenberger, H. Leonhardt, *Angew. Chem. Int. Ed.* **2015**, *54*, 13787–13791; *Angew. Chem.* **2015**, *127*, 13992–13996; d) B. Eddé, J. Rossier, J.-P. L. Caer, E. Desbruyères, F. Gros, P. Denoulet, *Science* **1990**, *247*, 83–85.
[9] a) D. Schumacher, O. Lemke, J. Helma, L. Gerszonowicz, V. Waller, T. Stoschek, P. M. Durkin, N. Budisa, H. Leonhardt, B. G. Keller, C. P. R. Hackenberger, *Chem. Sci.* **2017**, *8*, 3471–3478; b) A. Banerjee, T. D. Panosian, K. Mukherjee, R. Ravindra, S. Gal, D. L. Sackett, S. Bane, *ACS Chem. Biol.* **2010**, *5*, 777–785; c) A. Rovini, G. Gauthier, R. Bergès, A. Kruczynski, D. Braguer, S. Honoré, *PLoS One* **2013**, *8*, e65694.
[10] a) P. Verdier-Pinard, E. Pasquier, H. Xiao, B. Burd, C. Villard, D. Lafitte, L. M. Miller, R. H. Angeletti, S. B. Horwitz, D. Braguer, *Anal. Biochem.* **2009**, *384*, 197–206; b) V. Redeker, *Methods Cell Biol.* **2010**, *95*, 77–103.
[11] T. Becker, A. Wiest, A. Telek, D. Bejko, A. Hoffmann-Röder, P. Kielkowski, *JACS Au* **2022**, *2*, 1712–1723.
[12] C. S. Hughes, S. Moggridge, T. Müller, P. H. Sorensen, G. B. Morin, J. Krijgsveld, *Nat. Protoc.* **2019**, *14*, 68–85.
[13] a) L. R. Heil, W. E. Fondrie, C. D. McGann, A. J. Federation, W. S. Noble, M. J. MacCoss, U. Keich, *J. Proteome Res.* **2021**, *21*,1382–1391; b) Y. Kawashima, H. Nagai, R. Konno, M. Ishikawa, D. Nakajima, H. Sato, R. Nakamura, T. Furuyashiki, O. Ohara, *J. Proteome Res.* **2022**, *21*, 1418–1427; c) V. Demichev, C. B. Messner, S. I. Vernardis, K. S. Lilley, M. Ralser, *Nat. Methods* **2020**, *17*, 41–44.
[14] a) P. Bieling, S. Kandels-Lewis, I. A. Telley, J. van Dijk, C. Janke, T. Surrey, *J. Cell Biol.* **2008**, *183*, 1223–1233; b) X. Song, F. Yang, X. Liu, P. Xia, W. Yin, Z. Wang, Y. Wang, X. Yuan, Z. Dou, K. Jiang, M. Ma, B. Hu, R. Zhang, C. Xu, Z. Zhang, K. Ruan, R. Tian, L. Li, T. Liu, D. L. Hill, J. Zang, X. Liu, J. Li, J. Cheng, X. Yao, *Nat. Chem. Biol.* **2021**, *17*, 1314–1323.
[15] a) A. Rovini, G. Gauthier, R. Bergès, A. Kruczynski, D. Braguer, S. Honoré, *PLoS One* **2013**, *8*, e65694; b) A. Bosson, J.-M. Soleilhac, O. Valiron, D. Job, A. Andrieux, M.-J. Moutin, *PLoS One* **2012**, *7*, e33490.
[16] X.-D. He, W. Gong, J.-N. Zhang, J. Nie, C.-F. Yao, F.-S. Guo, Y. Lin, X.-H. Wu, F. Li, J. Li, W.-C. Sun, E.-D. Wang, Y.-P. An, H.-R. Tang, G.-Q. Yan, P.-Y. Yang, Y. Wei, Y.-Z. Mao, P.-C. Lin, J.-Y. Zhao, Y. Xu, W. Xu, S.-M. Zhao, *Cell Metab.* **2018**, *27*, 151–166.e6.
[17] C. S. Hughes, S. Foehr, D. A. Garfield, E. E. Furlong, L. M. Steinmetz, J. Krijgsveld, *Mol. Syst. Biol.* **2014**, *10*, 1–10.
[18] a) M. A. Tischfield, E. C. Engle, *Biosci. Rep.* **2010**, *30*, 319–330; b) T. J. Hausrat, J. Radwitz, F. L. Lombino, P. Breiden, M. Kneussel, *Dev. Neurobiol.* **2021**, *81*, 333–350; c) P. Guedes-Dias, E. L. F. Holzbaur, *Science* **2019**, *366*, eaaw9997.
[19] a) V. Busskamp, N. E. Lewis, P. Guye, A. H. Ng, S. L. Shipman, S. M. Byrne, N. E. Sanjana, J. Murn, Y. Li, S. Li, M. Stadler, R. Weiss, G. M. Church, *Mol. Syst. Biol.* **2014**, *10*, 760; b) E. Korytiaková, E. Kamińska, M. Müller, T. Carell, *Angew. Chem. Int. Ed.* **2021**, *60*, 16869–16873; c) T. Becker, C. Cappel, F. D. Matteo, G. Sonsalla, E. Kaminska, F. Spada, S. Cappello, M. Damme, P. Kielkowski, *iScience* **2021**, *24*, 103521.
[20] E. Arbely, J. Torres-Kolbus, A. Deiters, J. W. Chin, *J. Am. Chem. Soc.* **2012**, *134*, 11912–11915.

Manuscript received: July 21, 2022
Revised manuscript received: October 10, 2022
Accepted manuscript online: October 11, 2022
Version of record online: November 9, 2022